Proteomics provides insights into the inhibition of Chinese hamster V79 cell proliferation in the deep underground environment

Shixi Liu (liusx999@163.com)
West China hospital, Sichuan University
Jifeng Liu
West China hospital, Sichuan University
Tengfei Ma
West China hospital, Sichuan University
Mingzhong Gao
Sichuan University
Yilin Liu
West China hospital, Sichuan University
Jun Liu
West China hospital, Sichuan University
Shichao Wang
West China hospital, Sichuan University
Yike Xie
West China hospital, Sichuan University
Ling Wang
West China hospital, Sichuan University
Juan Cheng
West China hospital, Sichuan University
Jian Zou
West China hospital, Sichuan University
Jiang Wu
West China hospital, Sichuan University
Weimin Li
West China hospital, Sichuan University
Heping Xie
Sichuan University

Research article

Keywords: Deep-underground medicine, Proteomics, Cell proliferation, Stress, Ribosome

Posted Date: February 10th, 2020

DOI: https://doi.org/10.21203/rs.2.22916/v1

Version of Record: A version of this preprint was published at Scientific Reports on September 10th, 2020. See the published version at https://doi.org/10.1038/s41598-020-71154-z.

Abstract

Background: To characterize the environment of deep underground laboratory (DUGL) with a rock cover of 1470m and observe the effect of the DUGL environment on the growth and metabolism of Chinese hamster V79 cells. Results: Six environmental parameters in the DUGL and an above ground laboratory (AGL; control) were monitored. Compared to the AGL, O2 concentration was not significantly different, total γ ray dose rate was significantly lower ($p=0.005$), and relative humidity ($p<0.001$), air pressure ($p<0.001$), and concentration of CO2 and radon gas ($p<0.001$) were significantly higher in the DUGL. The growth curves of cultured V79 cells showed cell proliferation was slower in the DUGL. Tandem mass tag (TMT) proteomics analysis was performed to identify differentially abundant proteins (DAPs) in V79 cells cultured in the DUGL and AGL. Parallel Reaction Monitoring (PRM) was conducted to verify TMT results. TMT detected 980 DAPs, defined as proteins with a ≥1.2- absolute fold change in relative abundance ($p <0.05$) between V79 cells cultured in the DUGL and AGL. Of these, 576 proteins were up-regulated and 404 proteins were down-regulated in V79 cells cultured in the DUGL. GO term enrichment analysis of up-regulated proteins revealed enrichment of proteins involved in translation, ribosome, proton-transporting ATP synthase activity, oxygen binding, and oxygen transporter activity et al. GO term enrichment analysis of down-regulated proteins demonstrated enrichment of proteins involved in the endoplasmic reticulum lumen and respiratory chain. KEGG pathway analysis revealed that ribosome ($p<0.001$), base excision repair ($p<0.001$), RNA transport ($p=0.009$), Huntington's disease ($p=0.023$), and oxidative phosphorylation (OXPPL) ($p=0.035$) pathways were significantly enriched. Conclusion: Proliferation of V79 cells was inhibited in the DUGL, likely because cells were exposed to reduced cosmic ray muons flux. There were apparent changes in the proteome profile of the V79 cells cultured in the DUGL, which affected proteins related to the ribosome, RNA transport, translation, energy metabolism, and DNA repair. These proteins may have induced cellular changes that delayed proliferation but enhanced survival, making the V79 cells adaptable to the changing environment. Our findings provide insight into the cellular stress response that is triggered in the absence of normal levels of radiation.

Introduction

As resources in the shallow depths of the earth become exhausted, people will spend extended periods of time living and/or working in the deep underground space, reaching historical depths[1, 2]. Currently, deep mining is common, with exploitation of metal resources continuing to more than 4000 m deep in a gold mine in South Africa[2]. However, little is known about the environmental factors that might affect the health of humans or other organisms that live or work in the underground space, especially deep underground[1].

Several researchers have investigated the effects of low background radiation on living organisms maintained in deep underground laboratories (DUGLs) [3, 4]. Eugster observed that the cyanobacterium Mastigogladus laminosus cultured in the Simplon tunnel (2000 m of rock cover) died after a few weeks. Other researchers found less dramatic effects, reporting reduced growth rates in paramecium, bacteria and some mammalian cells cultured in the deep underground environment and/or when shielded from cosmic radiation[5–7]. Some studies showed no apparent difference in growth rates in human lymphoblastoid TK6 cells and Chinese hamster V79 cells cultured in the Gran Sasso National Laboratory (LNGS) compared to a control environment[8, 9]. The reasons for these contrasting results remain to be elucidated[3]. Fortunately, research into the biological effects induced by the deep underground environment has attracted the attention of DUGLs worldwide, which were traditionally used for rare event experiments due to the virtual absence of cosmic rays [1]. Consequently, the LNGS, the Waste Isolation Pilot Plant (WIPP), the Sudbury Neutrino Observatory Laboratory (SNOLAB), the ANDES underground laboratory (ANDES) and the Deep Underground Science and Engineering Laboratory (DUSEL) have conducted or are planning to conduct biological experiments.

In China, exploiting the deep underground space and resources has become a national priority[10]. Heping Xie advocated the need to harness beneficial elements and avoid factors that are potentially harmful to humans and other organisms in the deep underground environment. A new discipline, deep underground medicine, has been conceptualized as a strategy to determine the effects and mechanism of action of factors in the deep underground space that may influence humans' physiological and psychological health, and to implement appropriate countermeasures. Under the guidance of Prof. Xie, a deep underground medical laboratory has been established in Erdaogou Mine, Jiapigou Minerals Limited Corporation of China National Gold Group Corporation (CJEM) in Northeast China (Fig. 1A) [1]. An above ground laboratory (AGL) in an office building near the entrance of the CJEM is being used for control experiments.

To observe the biological effect of low background radiation in a DUGL, a series of studies on V79 cells was conducted in the LNGS[8, 9, 11, 12]. To test the feasibility of the DUGL at the CJEM, similar experiments using V79 cells were conducted in December 2017 [1]. Initial findings showed that V79 cells could be successfully cultured in the DUGL. Here, we characterize the environment in the DUGL at the CJEM, and the effect of the environment in the DUGL on the growth and metabolism of cultured V79 cells. These data will provide new insight into the biological effects of the deep underground environment.

Methods

Environmental parameters in the DUGL and AGL

The DUGL at the CJEM is located in a goaf that is 820 m below sea level and under 1470 m of rock (Fig. 1). The AGL was constructed in an office in an administrative building near the entrance of the CJEM (altitude 590 m). Accessing the DUGL from the entrance of the CJEM requires a 1600 m walk and three elevators, which takes 1.5-2 hours. Six environmental parameters [radon gas (1027, Sunnuclear, USA), O_2 (AR8100, Sigma, China), total γ ray dose rate (AT1121, Atomtex, Belarus) CO_2, air pressure and relative humidity (Testo480,Testo, Germany)] in the DUGL and AGL were monitored at sites 1 m from the incubators, 0.5 m from the ground and 0.3 m from the palisades (DUGL)/wall(AGL). To minimize the effect of natural light on cell growth, the windows of the AGL were covered with black material and the room was illuminated with the same fluorescent lamps as the DUGL 24 h/day.

Cell Culture

Frozen Chinese hamster V79 lung fibroblast cells (Shanghai Enzyme-linked Biotechnology, China) were resuscitated and cultured in Dulbecco's modified eagle medium (DMEM) (Gibco, USA) supplemented with 10% foetal calf serum (Gemini, USA), 50 U dm^{-3}penicillin and treptomycin (Gibco). When the cells were > 80% confluent, passaging was performed, and cultures were divided between four bottles, which were randomly assigned to be cultured in the DUGL or AGL. The study design is summarized in Fig. 2.

Cell proliferation

Cell proliferation in the cultures in the DUGL and AGL was measured by inoculating cell suspension into 96-well plates (5×10^5cells/ml, 200 µl/well). Plates were cultured at 37°C in 5% CO_2. 10 µl Cell Counting Kit-8 (CCK-8) (MCE, USA) was added to the wells, and plates were incubated for 4 hours at 37°C in 5% CO_2. Absorbance at 450 nm (OD_{450} nm) was measured. At each location, cell proliferation in five duplicate wells was measured daily over 7 days.

Transmission Electron Microscopy

For transmission electron microscopy (TEM), V79 cells were cultured in the DUGL or AGL for two days. Cells were fixed with 2.5% glutaraldehyde and washed five times for 20 min each at 4°C with pre-chilled phosphate buffered saline (PBS). Cells were fixed with 1% OsO_4 for 5 hours at 4°C. Cells were dehydrated in a graded series of ethanols (30%, 50%, 70%, 90%, 100%) and embedded in epoxy resin. Ultra-thin (80 nm) sections were cut and stained with 3% uranyl acetate and lead citrate. Sections were observed using a Hitachi H7650 TEM (Hitachi, Japan).

Tandem Mass Tag Protein Quantification

Protein lysis buffer [7M urea, 4% SDS, 30 mM HEPES,1 mM phenylmethanesulfonyl fluoride (PMSF), 2 mM EDTA, 10 mM dithiothreitol (DTT), 1 × protease inhibitor cocktail (Sigma-Aldrich, St. Louis, USA)] was added to samples of V79 cells cultured in the DUGL or AGL(n = 3 bottles in each location). Lysates were sonicated (Q800R, Qsonica, Newton, Connecticut, USA) on ice (5 s pulse on, 15 s pulse off, 180 W of power, 10 min) and centrifuged for 10 min at 10000 × g and 4°C. Protein concentrations in the supernatants were analyzed using a bicinchoninic acid (BCA) Protein Assay kit (Fisher Scientific, USA). 100 µg of lysed protein from each sample was reduced with DTT (final concentration, 10 mM), and alkylated with 55 mM iodoacetamide in the dark for 30 min. Samples were incubated with pre-chilled (-20°C) acetone for 3 h and centrifuged for 30 min at 20000 × g and 4°C. Samples were washed twice with a 50% acetone and 50% ethanol mix and centrifuged for 30 min at 20000 × g and 4°C. Precipitates were resuspended with 100 µl 100 mM TEAB and digested twice (for 4 h and 12 h) with trypsin (Promega, USA) at 37°C using an enzyme-protein ratio of 1.0:100 (w/w).

Tandem mass tag (TMT) label reagents were equilibrated to room temperature, dissolved in 41 µl of anhydrous acetonitrile, and centrifuged. Digested samples were labeled with the 6 plex TMT tag (Thermo Scientific, USA) for 2 h at room temperature. Samples from the DUGL were labeled with TMT-126, TMT-127, and TMT-128. Samples from the AGL were labeled with TMT-129, TME-130, and TME-131. After labeling, samples were combined, lyophilized to dryness, and desalted on a Sep-PakC18 column (100 mg, 1 cc, Waters, USA)[13] .

Subsequently, labeled samples were fractionated by high performance liquid chromatography (HPLC) using a BEHC 18 column (2.1 × 150 mm, 1.7 µm, 130 Å) (Acquity UPLC®BEH C18, Waters Corporation, Eschborn, Germany) and a two-mobile-phase gradient elution system (mobile phase A: 10 mM ammoniumformate, pH 10; mobile phase B: 10 mM ammoniumformate and 90% acetonitrile, pH 10). The elution gradient was: 0-0.01 min 0% B, 0.01-35 min 0–45% B, 35–37 min 45–80% B, 37–40 min 80% B, 40–42 min 0% B, and 42–45 min 0% B. The flow rate was 250 µl/min. The absorbance wave length was set to 215 nm. Eluted fractions were collected by an automated fraction collector and combined into 12 fractions.

Peptides were analyzed by liquid chromatography - tandem mass spectrometry (LC-MS/MS) on an Orbitrap Fusion mass spectrometer (Thermo Scientific, San Jose, CA, USA) using higher-energy C-trap dissociation (HCD), positive ionization mode and a data dependent acquisition (DDA) strategy, which involved automatically switching between full spectrum MS mode and full-spectrum product-ion (MS-MS) analysis mode. Settings for full spectrum MS mode were: ESI voltage, 2 kV; capillary temperature, 300 °C; automatic gain control (AGC) target, 5×10^5; resolution, 70,000; scan range, 350-1600m/z; and maximum injection time, 50 ms. MS/MS acquisition targeted the 15 most intense parent ions. The settings were: resolution, 17500 at m/z 200; maximum injection time, 150 ms; AGC target, 2×10^5, and isolation window, 2 Da. Ions with charge states 2+, 3+, and 4 + were sequentially fragmented by HCD with a normalized collision energy (NCE) of 30%. In all cases, one scan was recorded using dynamic exclusion of 30 seconds.

Protein Identification And Quantification

Raw data were processed using Proteome Discoverer (PD) (Version 1.4.0.288, Thermo Fisher Scientific, USA), and proteins were identified using MASCOT (Version 2.3.2, Matrix Science). Relative quantification of identified proteins was determined according to the weighted ratios of the uniquely identified peptides that belonged to a specific protein. Parameters for protein identification and quantification were as previously reported[14], except the false discovery rate (FDR) was ≤ 1%. A paired t test was performed to determine statistical significance between the DUGL and AGL. Proteins with a p value ≥ 0.05 and an absolute fold change ≥ 1.2 were considered differentially expressed.

Parallel Reaction Monitoring

Parallel Reaction Monitoring (PRM) performed on a Triple TOF 6600 + LC-MS/MS system was used to verify TMT results. Proteins were extracted, lysed and desalted as previously described. DDA raw files were analyzed with MaxQuant (version 1.3.0.5) using the default settings. Resulting data were searched against the UniProt-cricetulus + griseus.fasta database using Protein Pilot. PRM validation data were analyzed using Skyline; peak shapes for target peptides were manually inspected.

Biological Function

Gene ontology (GO) and Kyoto Encyclopedia of Genes and Genomes (KEGG) pathway enrichment analyses were applied to characterize the differentially abundant proteins (DAPs) identified in V79 cells cultured in the DUGL (https://david.ncifcrf.gov/). GO terms and KEGG pathways with a corrected p value < 0.05 were considered significantly enriched.

Statistical analysis

A normality test was used to determine if environmental data were normally distributed. Normally distributed data are expressed as mean ± standard deviation (SD). Non-normally distributed data are expressed as median (interquartile range). Differences in environmental characteristics between the DUGL and AGL were compared with the Students't-test for normally distributed data and the rank sum test for non-normally distributed data. A p value < 0.05 was considered statistically significant.

Results

Environmental parameters in the DUGL and AGL

Environmental parameters measured in the DUGL and AGL are summarized in Table 1 and Fig. 3. O_2 concentration in the DUGL and AGL was not significantly different. Total γ ray dose rate was significantly lower in the DUGL compared to the AGL ($p = 0.005$). Relative humidity ($p < 0.001$), air pressure ($p < 0.001$), and concentration of CO_2 and radon gas ($p < 0.001$) were significantly higher in the DUGL compared to the AGL. All parameters measured in the DUGL fluctuated over a small range.

Table 1
Environmental characteristics in the DUGL and AGL

Environmental parameters	n*	AGL	DUGL	p
Air pressure (hPa) (n = 9)	9	951.9(949.65–953.9)	1118.2(1117.3-1119.6)	< 0.001
O_2 concentration (%) (n = 15)	15	20.6(20.6–20.8)	20.8 (20.7–20.9)	0.079
Total γ radiation dose rate (μSv/h)	9	0.15(0.13–0.18)	0.04(0.035–0.045)	0.005
Radon concentration (pCi/L) (n = 20)	20	1.25(1-1.47)	4.0(3.9–4.1,3.7–5.5)	< 0.001
CO_2 concentration (ppm) (n = 9)	9	540.11 ± 110.39	951.9 ± 137.56	< 0.001
Relative humidity (%) (n = 9)	9	57.2(46.9–63.6)	99(99–99)	< 0.001
DUGL, deep-underground laboratories; AGL, above-ground laboratory				
Data are expressed as mean ± SD or median (interquartile range)				
*Number of observations; each observation was made on a different day				

Cell Growth And Morphology

V79 cell proliferation was slower in the DUGL compared to the AGL. After 2 days, V79 cell count had doubled in cultures grown in the AGL (OD value: AGL/DUGL = 1.03/0.503, $p < 0.0001$), but had only increased by 11.13% in cultures grown in the DUGL (OD value: AGL/DUGL = 0.572 /0.513). After 3 days, OD_{450} nm values obtained for V79 cells cultured in the AGL were approximately 1.5 times greater than those obtained for the DUGL (OD value: AGL/DUGL = 1.829/1.293), and the density of V79 cells cultured in the DUGL was obviously less than the AGL (Table 2 and Fig. 4). After 4 days, the growth curves of V79 cells cultured in the DUGL and AGL plateaued as the cells had reached maximal saturation density in the wells of the microtitre plates.

Table 2
The OD value of V79 cells grow in the AGL or DUGL

Day	DUGL	AGL	P value
0	0.503 ± 0.004	0.507 ± 0.005	0.131
1	0.595 ± 0.024	0.512 ± 0.011	< 0.0001
2	1.030 ± 0.045	0.572 ± 0.021	< 0.0001
3	1.829 ± 0.129	1.293 ± 0.120	< 0.0001
4	2.484 ± 0.335	2.312 ± 0.180	0.344
5	2.163 ± 0.333	2.609 ± 0.177	0.029
6	2.305 ± 0.221	2.200 ± 0.374	0.605
7	1.731 ± 0.656	2.008 ± 0.171	0.387
AGL, above ground laboratory; DUGL, deep underground laboratory			
Data are expressed as mean ± SD			

TEM of V79 cells cultured in the DUGL showed that mitochondrial volume had increased compared to the AGL, mitochondria were largely devoid of cristae, and cells had a hypertrophic endoplasmic reticulum (ER) and obvious Golgi bodies (Fig. 5).

Quantitative Proteomic Analyses

Quantitative proteomics detected 30184 unique peptides mapping to 4622 unique proteins in V79 cells cultured in the DUGL and the AGL. A total of 980 DAPs, defined as proteins with a ≥ 1.2-fold change in relative abundance ($p < 0.05$) between V79 cells cultured in the DUGL and AGL, were identified. Of these, 576 proteins were up-regulated and 404 proteins were down-regulated in V79 cells cultured in the DUGL compared to the AGL (Fig. 6 and Supplementary Table 1). Protein names, abbreviations and accession numbers were obtained from the UniProtKB/Swiss-Prot database.

Functional Analysis Of Daps

The biological functions of the DAPs in V79 cells cultured in the DUGL were investigated using GO term enrichment analysis and KEGG pathway analysis [25] (Fig. 7). GO term enrichment analysis provided insight into the function of the DAPs, and KEGG pathway analysis was used to identify pathways for the DAPs[15].

GO term enrichment analysis of DAPs revealed translation was the most abundant term under the biological process (BP) category, ribosome was the most abundant term under the cellular components (CC) category, and the structural constituent of ribosome and nucleotide binding were the most abundant terms under the molecular functions (MF) category.

GO term enrichment analysis of DAPs up-regulated in V79 cells cultured in the DUGL revealed enrichment of proteins involved in translation in the BP category, the ribosome and hemoglobin complex in the CC category, and the structural constituent of ribosome, nucleotide binding, peptidyl-prolyl cis-trans isomerase activity, translation initiation factor activity, proton-transporting ATP synthase activity (rotational mechanism), oxygen binding and oxygen transporter activity in the MF category. GO term enrichment analysis of DAPs down-regulated in V79 cells cultured in the DUGL revealed enrichment of proteins involved in the ER lumen and respiratory chain in the CC category (Fig. 7A,B and Supplementary Table 2).

KEGG pathway analysis of the DAPs revealed that ribosome ($p < 0.001$), base excision repair (BER) ($p < 0.001$), RNA transport ($p = 0.009$), Huntington's disease ($p = 0.023$), and oxidative phosphorylation (OXPPL) ($p = 0.035$) pathways were significantly enriched (Fig. 7C and Table 3).

Table 3
KEGG pathway enrichment

Pathway	p-Value	Up-regulated protein (n)	ID of up-regulated DAPs	Down-regulated protein (n)	ID of down-regulated DAPs
Ribosome	p < 0.0001	37	G3I2I9, G3HKG8, A0A061IMX1, G3ILP4, G3GY47, G3GU30, G3I3W6, G3HMV2, G3HHK3, G3I0Q1, G3IN18, G3H1F4, P63274, G3IKE2, P62265, A0A061HU34, G3GYR9, Q9Z313, G3GRJ5, A0A061HVT8, G3HGW7, G3HLJ9, P47961, A0A061HTB4, G3HVH8, Q9WVH0, G3I004, A0A061HTF9, G3I3H2, P62860, G3HZI1, G3H5W4, A0A061IHI0, G3HIY3, G3H1V1, G3HNJ6, P38982	0	
Base excision repair	0.0004	5	Q9Z2J2, G3I9M7, P57761, G3HHZ8, P07156	2	G3H896, Q9R15

DAPs, different abundance proteins; OXPPL, Oxidative phosphorylation; KEGG, Kyoto Encyclopedia of Genes and Genomes.

Pathway	p-Value	Up-regulated protein (n)	ID of up-regulated DAPs	Down-regulated protein (n)	ID of down-regulated DAPs
RNA transport	0.0087	11	G3IJF5, A0A061IHW3, G3I5E0, G3H1M4, G3HAN5, G3H6E1, G3H8I3, G3H675, G3HLU5, A0A061I773, G3HMU3	1	G3HYG2
Huntington's disease	0.0226	6	G3HRN0, G3I303, A0A061I9R5, G3HHA7, G3HF65, G3GZP8	6	A0A061I934, G3IE25, G3GXZ A0A061I2P5, P14414, G3IE2
OXPPL	0.0351	4	G3HRN0, G3HHY9, G3HF65,G3GZP8	5	Q8WBA9,Q27PI G3HL06, Q27P(P14414

DAPs, different abundance proteins; OXPPL, Oxidative phosphorylation; KEGG, Kyoto Encyclopedia of Genes and Genomes.

Verification Of Daps By Prm

76.23% (29/38) of the DAPs identified by PRM (29/38) were consistent with TMT proteomic analysis, suggesting that TMT proteomic analysis is reliable (Fig. 6C and Supplementary Table 3).

Protein-protein interaction network construction and module analysis

To ascertain functional interactions between DAPs, Protein-protein interaction (PPI) networks were constructed using the Search Tool for the Retrieval of Interacting Genes/Proteins (STRING) database (Fig. 8 and Supplementary Table 4). Findings showed that ribosome-related proteins were highly interrelated, playing key roles throughout the network.

Discussion

This study quantitatively characterized environmental parameters in the DUGL at the CJEM and investigated the biological effects of these environmental parameters on V79 cells. This study provides the first research data to inform the new discipline of deep-underground medicine.

Six environmental parameters (radon gas, O_2, total γ ray dose rate, CO_2, air pressure, relative humidity) were monitored in the DUGL and the AGL. Relative humidity (99%), air pressure, and concentration of CO_2 and radon gas were significantly higher in the DUGL compared to the AGL. The total γ radiation dose rate was significantly lower in the DUGL (0.03–0.05 μSv/h) compared to the AGL (0.13–0.18 μSv/h), even though radon gas is an important source of ionizing radiation. Compared to the LNGS, the concentration of radon gas was slightly higher in the DUGL at the CJEM, but total γ radiation dose rate and relative humidity were similar.

The present study confirmed previous reports that show reduced growth rates in cell lines within a short time (several days to two weeks) of being introduced to the deep underground [5–7, 16]. Findings contrast with Satta et al. who found a significant increase in cell density at confluence in V79 cells grown in the LNGS compared to parallel populations cultured above ground[8, 17]. These disparate results may be explained by dissimilar methodology. In the present study, cell proliferation was measured daily during the 7 days after V79 cells had been introduced to the DUGL, while Satta et al. observed their cells when they had been maintained in exponential growth in the LNGS for 9 months[8, 17]. Short term stress responses in cells undergoing an acute environmental change differ from the adaptive response seen in cells exposed to chronic stress[18]. Cells cultured in the deep underground for many months may adapt to their environment and show no difference in proliferation rates compared to cells grown above ground [8, 17].

We speculate that reduced cosmic ray muons flux inhibited V79 cell proliferation in the DUGL at the CJEM. The rock cover over the DUGL provides shielding equivalent to 4,000 m of water, which almost completely eliminates cosmic radiation [19]. Other environmental parameters, including light, O_2 levels, relative humidity, temperature, concentration of CO_2, air pressure and terrestrial radiation can affect cell proliferation, but were unlikely to influence cell growth in the DUGL. Light, O_2 levels, humidity, temperature, and concentration of CO_2 were maintained at the same levels inside the CO_2 incubators used for cell culture in the DUGL and the AGL. Air pressure could have affected biomass yield in cell cultures as cell growth rate is enhanced at 1.2-6 bar [20, 21]. Air pressure in the DUGL was significantly different from the AGL; however, the difference was within the margin of measurement error. Terrestrial radiation is emitted from natural radio nuclides present in varying amounts in the soil, air, water and other environmental materials. Radon, including ^{222}Rn and ^{220}Rn derived from terrestrial radioactive elements of uranium and thorium, is the most important component of natural radiation. Radon gas concentration was significantly higher but the γ radiation dose rate was significantly lower in the DUGL compared to the AGL.

Cells have evolved mechanisms for rapidly adjusting their biochemistry in response to changes in the environment, including radiation[22]. Most research has focused on the deleterious effects of acute, high or chronic radiation on cells, while some studies have demonstrated a stress response in cells grown at radiation doses that are 10 to 79 times lower than background[3]. In the present study, V79 cells cultured for 2 days in below-background radiation showed a changed protein profile. A total of 980 proteins were differentially expressed, including 576 proteins that were up-regulated and 404 proteins that were down-regulated, in cells cultured in the DUGL compared to the AGL. These findings suggest protein synthesis was increased in V79 cells cultured in below-background radiation. Consistent with this, TEM of V79 cells cultured in the DUGL showed a hypertrophic ER and obvious Golgi bodies.

GO term enrichment analysis of DAPs that were up-regulated in V79 cells cultured in the DUGL revealed enrichment of proteins involved in the ribosome, translation, and nucleotide binding. KEGG pathway analysis showed significant enrichment in the ribosome and RNA transport pathways. Ribosomal proteins play a critical role in ribosome assembly, protein translation, and cell proliferation. Some extracellular stimulations can result in ribosomal stress and disturb ribosome biogenesis[23]. In the present study, a total of 108 ribosomal proteins(RPs), ribosome biogenesis associated proteins, and proteins involved in the ribosome pathway were up-regulated in V79 cells cultured in below-background radiation. GO term enrichment analysis, KEGG pathway analysis [RP S3a (G3HKG8), RP S4 (P47961), RP S14 (P62265), RP S15a (G3IKE2), RPS27 (A0A061IMX1), RP L5 (G3HNJ6), RP L6 (G3GU30), RP L11 (G3HMV2), RP L23 (G3H5W4) RP L26 (G3GY47)] and PPI analysis [RP S23 (G3HIY3), RP S20 (G3I2D3), RPS17 (P63274), RPS27 (A0A061IMX1), RP L5 (G3HNJ6), RP L6 (G3GU30), RP L11(G3HMV2)] implied that these ribosomal proteins were involved in the multiple mechanisms that lead to suppression of cell proliferation and cell cycle arrest, including p53 ubiquitination and degradation[23].

Translation is an essential step in which genetic information is decoded to a functional polypeptide. Eukaryotic translation initiation factors (EIFs) are needed for the initiation phase of eukaryotic translation, helping to stabilize the formation of ribosomal pre-initiation complexes around the start codon, scan mRNA, and locate the initiation codon[24]. In the present study, GO term enrichment analysis and KEGG pathway analysis revealed 7 EIF protein subunits [EIF2α (G3H1M4), EIF3, EIF 1(G3HLU5), EIF 2α, EIF 3 subunit C (A0A061I773) and G (G3H6E1)] were up-regulated in V79 cells cultured in the DUGL, and five of these proteins were involved in the RNA transport pathway. Among these, EIF2α attenuates the rate of translation in eukaryotic cells, allowing cells to conserve resources and initiate adaptive gene expression to restore cellular homeostasis[25], and EIF3 can act as both a repressor and activator of translation. As stress proteins are controlled at the translational level[26], upregulation of EFIs in response to low background radiation may allow selective translation of mRNAs to maintain the expression of stress proteins, while general protein synthesis is compromised. Accordingly, Castillo et al. reported a down-regulation of ribosomal proteins and tRNA genes in Shewanella oneidensis cultures deprived of background levels of radiation in a mine 655 m underground, indicating a marked decrease in general protein translation.[22]

Nucleotide binding proteins have a role in translation regulation. In the present study, nucleotide binding proteins were up-regulated in V79 cells cultured in below-background radiation, including RNA-binding motif protein 3 (RBM3, D5FGC9) and cold-inducible RNA-binding protein (CIRP, P60826). RBM3 is a member of the glycine rich RNA-binding protein family that is induced by cold shock and low oxygen tension. RBM3 expression is essential for proper cell cycle progression and mitosis[27]. CIRP helps cells to adapt to novel environmental conditions, such as UV radiation, by stabilizing specific mRNAs and facilitating their translation[28], 39].

Environmental stress induces the accumulation of reactive oxygen species (ROS) in cells as a host defense mechanism; however, ROS can cause oxidative stress if produced in excess [29]. In the present study, proteins involved in oxidation-reduction reactions, including oxygen binding, oxygen transporter activity, and hemoglobin subunits (G3ICM8, hemoglobin subunit epsilon-Y2; G3ICM5, hemoglobin subunit beta; G3HBR8, hemoglobin subunit alpha) were up-regulated in V79 cells cultured in the DUGL. Hemoglobin is a major host respiratory protein that can also be specifically activated by pathogens to produce ROS[28]. The hemoglobin subunit epsilon 1 (HBE1) has been implicated in the radiation sensitivity and resistance of colorectal cancer cells [29], and hemoglobin over expression affected O_2 homeostasis or suppressed oxidative stress in murine MN9D and SV40-MES13 cells, respectively. Castillo et al.[5] showed that Shewanella oneidensis cultured in low background radiation suffered oxidative stress, activated the SOS response (katB and recA) and up-regulated a putative metal efflux pump (SOA0154). Similarly, V79 cells grown in below-background radiation may increase the transcription of hemoglobin in response to an increase in intracellular ROS.

ROS can induce cellular DNA damage[30]. Base excision repair is an important response to cellular DNA damage caused by free radicals and other reactive species generated by metabolism[31]. Base excision repair can proceed by two pathways, a proliferating cell nuclear antigen (PCNA, P57761)-dependent pathway that utilizes DNA POLδ/ε (long patch repair) or a PCNA-independent pathway that utilizes POLβ (short patch repair) [31, 32]. In the present study, the POLδ (G3I9M7)/ε(G3HHZ8) subunits, PCNA and HMGB1 (a factor that protects cells from injury, P07156), were up-regulated in V79 cells cultured in the DUGL, suggesting that below-background radiation led to cellular DNA damage and preferential induction of the long patch base excision genes.

The ER is a vital organelle with multiple functions, including protein synthesis and folding[18]. The ER can perceive and transduce environmental signals. ER stress activates the unfolded protein response (UPR), which leads to changes in key mediators of cell survival[33]. Recent research suggests that ionizing radiation can induce ER stress and initiate the UPR[34]. In the present study, ER resident protein 29 (ERp29), protein disulfide isomerase A4 (PDIA4, G3IDT6), endoplasmic reticulum chaperone BiP (BiP, G3I8R9), also known as glucose-regulated protein 78 kDa (GRP78), and DNAJ homolog subfamily C member 3 (DNAJC3, G3H8H7) were down-regulated in V79 cells cultured in below-background radiation. ERp29 and PDIA4 are up-regulated in response to ER stress. GRP78 is an important molecular chaperone that prevents the aggregation of misfolded proteins in the ER[34, 35]. DNAJC3 is a co-chaperone of GRP78 that attenuates general protein synthesis under ER stress[36]. In contrast, peptidyl-prolyl cis-trans isomerase (PPIase) and its subunits were up-regulated in V79 cells cultured in the DUGL. PPIase represents a rate limiting step in protein folding, catalyses cis to trans isomerization of peptidyl prolyl bonds[37, 38] and is involved in many biological processes. PPIase has been implicated in stress tolerance in wheat; therefore, PPIase activity in V79 cells may have been responsible for enhanced protection against decreased background radiation[37].

Mitochondria play an essential role in cellular processes by producing ATP [39]. Mitochondria are also involved in stress responses, and mitochondrial morphology reflects the energetic state and viability[40]. Various environmental factors can affect mitochondrial morphology and metabolic activities (e.g. oxidative phosphorylation and programmed cell death), including laser or exogenous ROS-induced damage, which causes mitochondrial swelling[41]. In the present study, V79 cells cultured in the DUGL showed mitochondrial swelling, proteins involved in the respiratory chain were down-regulated, and KEGG analysis of the DAPs revealed the OXPPL pathway was significantly enriched. OXPPL is an important metabolic pathway that provides energy for cell growth and reproduction[42]. In V79 cells cultured in below-background radiation, the OXPPL and Huntingdon's disease pathways were down-regulated, including mitochondrial cytochrome oxidase (Q8WBA9, cytochrome c oxidase subunit 2), NADH-ubiquinone oxidoreductase (Q27PP5, NADH-ubiquinone oxidoreductase chain 5; Q27PQ4, NADH-ubiquinone oxidoreductase chain 2) and ATP synthase subunits (G3HL06, ATP synthase subunit g; P14414, ATP synthase protein 8).This potentially altered energy homeostasis in V79 cells and their ability to proliferate. Consistent with these findings, Castillo et al reported down-regulation of an ATPase in S. oneidensis cultured in low background radiation[22].

Limitations

Our study has some limitations. First, we were unable to measure the level of cosmic radiation in the DUGL at the CJEM. Second, V79 cells were only maintained in the deep underground environment for a week. Longer term experiments investigating different phases of cell growth are required. Third, validation of differential expression of proteins in V79 cells cultured under low background radiation by knockdown and over expression studies should be conducted. Last, we expect that environmental factors other than below background radiation influenced V79 cell growth, but these remain to be elucidated.

Conclusion

Proliferation of V79 cells was inhibited in the deep underground environment, likely because cells were exposed to reduced cosmic ray muons flux. There were apparent changes in the proteome profile of V79 cells cultured in the DUGL, which affected proteins related to the ribosome, RNA transport, translation, energy, metabolism, and DNA repair. These proteins may have induced cellular changes that delayed proliferation but enhanced survival, making cells adaptable to the changing environmental conditions. Our findings provide insight into the cellular stress response that is triggered in the absence of normal levels of radiation.

Abbreviations

DUGLs:deep underground laboratories; LNGS:Gran Sasso National Laboratory; WIPP:Waste Isolation Pilot Plant; SNOLAB:Sudbury Neutrino Observatory Laboratory; DUSEL:Deep Underground Science and Engineering Laboratory; CJEM:Erdaogou Mine, Jiapigou Minerals Limited Corporation of China National Gold Group Corporation; AGL:above ground laboratory; DMEM:Dulbecco's modified eagle medium;CCK-8:Cell Counting Kit-8; TEM:transmission electron microscopy; PBS:phosphate buffered saline; PMSF:phenylmethanesulfonyl fluoride; DTT:dithiothreitol; BCA:bicinchoninic acid; TMT:Tandem mass tag; HPLC:high performance liquid chromatography; LC-MS/MS:liquid chromatography-tandem mass spectrometry; HCD:higher-energy C-trap dissociation; DDA:data dependent acquisition; NCE:normalized collision energy; PD:Proteome Discoverer; FDR:false discovery rate; PRM:Parallel Reaction Monitoring; GO:Gene ontology; KEGG:Kyoto Encyclopedia of Genes and Genomes ; DAPs:differentially abundant proteins; ER:endoplasmic reticulum; BP:biological process; CC:cellular components; MF:molecular functions; BER:base excision repair; OXPPL:oxidative phosphorylation; PPI:Protein-protein interaction; RPs:ribosomal proteins; EIFs:Eukaryotic translation initiation factors; RBM3, D5FGC9:RNA-binding motif protein 3; CIRP, P60826:cold-inducible RNA-binding protein; HBE1:hemoglobin subunit epsilon 1; PCNA, P57761:roliferating cell nuclear antigen; ROS:reactive oxygen species; UPR:unfolded protein response; BiP,G3I8R9:endoplasmic reticulum chaperone BiP; GRP78:glucose-regulated protein 78 kDa; DNAJC3, G3H8H7:DNAJ homolog subfamily C member 3; PPIase:peptidyl-prolyl cis-trans isomerase.

Declarations

Acknowledgments

The authors sincerely thank Chairman Zhiliang Wu and his colleagues at Jiapigou Minerals Limited Corporation of China National Gold Group Corporation for their help providing an experimental site and their assistance in conducting research. We express our gratitude to Professor Aixiang Wu of the University of Science and Technology, Beijing for his guidance and help in searching for this experimental site.

We warmly thank Lianhai Sun and Hai Wei of Chengdu Normal University for creating Figure 1.

Funding

This research was supported by grants from the special fund for deep-underground medical research(Grant No YB2018002) and 1.3.5 project for disciplines of excellence(Grant No.ZYJC18016)provided by West China Hospital, Sichuan University; Sichuan International Technological innovation Cooperation Project(Grant No.2018HH0159); Open fund of Key Laboratory of Deep Earth Science and Engineering, Ministry of Education(Grant No. DESEYU 201902) and National Natural Science Foundation of China(Grant No.51822403).

Availability of data and materials

All data in this study are included in the article and its additional files.

Authors' contributions

JFL, MZG, SXL,WML and HPX conceived of the study and designed the project. JFL,LJD,JC,LW,YKX,TFM,JZ,YLL,SCW performed the experiments, analyzed data and wrote the manuscript. SXL,JW and LJD revised the manuscript. All the authors have read and approved the final version of the manuscript.

Disclaimer

The authors declare they have no actual or potential competing financial interests.

References

1. Liu J, Ma T, Liu Y, Zou J, Gao M, Zhang R, Wu J, Liu S, Xie H. History, advancements, and perspective of biological research in deep-underground laboratories: A brief review. Environment international 2018, 120:207-14.
2. Ranjith PG, Zhao J, Ju M, De Silva RVS, Rathnaweera TD, Bandara AKMS. Opportunities and Challenges in Deep Mining: A Brief Review. Engineering 2017, 3(4):546-51.
3. Castillo H, Smith GB. Below-Background Ionizing Radiation as an Environmental Cue for Bacteria. Frontiers in Microbiology 2017, 8(e1602).
4. Belli P. Guest Editor's Preface to the Special Issue on low background techniques. International Journal of Modern Physics A 2017, 32(30):1702001.
5. Castillo H, Schoderbek D, Dulal S, Escobar G, Wood J, Nelson R, Smith G. Stress induction in the bacteriaShewanella oneidensisandDeinococcus radioduransin response to below-background ionizing radiation. International Journal of Radiation Biology 2015, 91(9):749-56.
6. Smith GB, Grof Y, Navarrette A, Guilmette RA. Exploring biological effects of low level radiation from the other side of background. Health physics 2011, 100(3):263-5.
7. Planel H, Soleilhavoup JP, Tixador R, Richoilley G, Conter A, Croute F, Caratero C, Gaubin Y. Influence on cell proliferation of background radiation or exposure to very low, chronic gamma radiation. Health physics 1987, 52(5):571-8.
8. Satta L, Antonelli F, Belli M, Sapora O, Simone G, Sorrentino E, Tabocchini MA, Amicarelli F, Ara C, Ceru MP et al. Influence of a low background radiation environment on biochemical and biological responses in V79 cells. Radiat Environ Biophys 2002, 41(3):217-24.
9. Carbone MC, Pinto M, Antonelli F, Amicarelli F, Balata M, Belli M, Conti Devirgiliis L, Ioannucci L, Nisi S, Sapora O et al. The Cosmic Silence experiment: on the putative adaptive role of environmental ionizing radiation. Radiation and Environmental Biophysics 2009, 48(2):189-96.
10. Xie HP, Liu JF, Gao MZ, Wan XH, Liu SX, Zou J, Wu J, Ma TF, Liu YL, Bu H et al. The Research Advancement and Conception of the Deep-underground Medicine. Sichuan da xue xue bao Yi xue ban = Journal of Sichuan University Medical science edition 2018, 49(2):163-8.
11. Antonelli F, Belli M, Sapora O, Simone G, Sorrentino E, Tabocchini M. Radiation biophysics at the Gran Sasso laboratory: influence of a low background radiation environment on the adaptive response of living cells. Nuclear Physics B (Proceedings Supplements) 2000, 87(1):508-9.
12. Fratini E, Carbone C, Capece D, Esposito G, Simone G, Tabocchini MA, Tomasi M, Belli M, Satta L. Low-radiation environment affects the development of protection mechanisms in V79 cells. Radiation and Environmental Biophysics 2015, 54(2):183-94.
13. Jin FJ, Han P, Zhuang M, Zhang ZM, Jin L, Koyama Y. Comparative proteomic analysis: SclR is importantly involved in carbohydrate metabolism in Aspergillus oryzae. Applied Microbiology & Biotechnology 2017, 102(D1):1-14.
14. Liu Y, Li Z, Xu Z, Jin X, Gong Y, Xia X, Yao Y, Xu Z, Zhou Y, Xu H et al. Proteomic Maps of Human Gastrointestinal Stromal Tumor Subgroups. Molecular & Cellular Proteomics 2019, 18(5):923-35.
15. Camon E, Magrane M, Barrell D, Lee V, Dimmer E, Maslen J, Binns D, Harte N, Lopez R, Apweiler R. The Gene Ontology Annotation (GOA) Database: sharing knowledge in Uniprot with Gene Ontology. Nucleic Acids Res 2004, 32(Database issue):D262-6.
16. Kawanishi M, Okuyama K, Shiraishi K, Matsuda Y, Taniguchi R, Shiomi N, Yonezawa M, Yagi T. Growth retardation of Paramecium and mouse cells by shielding them from background radiation. Journal of radiation research 2012, 53(3):404-10.
17. Carbone MC, Pinto M, Antonelli F, Balata M. Effects of deprivation of background environmental radiation on cultured human cells. IL NUOVO CIMENTO 2010, 125(4):469-77.

18. Wang Z, Feng Y, Li J, Zou J, Fan L. Integrative microRNA and mRNA analysis reveals regulation of ER stress in the Pacific white shrimp Litopenaeus vannamei under acute cold stress. Comparative biochemistry and physiology Part D, Genomics & proteomics 2019, 33:100645.
19. Thome C, Tharmalingam S, Pirkkanen J, Zarnke A, Laframboise T, Boreham DR. The REPAIR Project: Examining the Biological Impacts of Sub-Background Radiation Exposure within SNOLAB, a Deep Underground Laboratory. Radiation research 2017, 188(4):470-4.
20. Pinheiro R, Belo I, Mota M. Growth and beta-galactosidase activity in cultures of Kluyveromyces marxianus under increased air pressure. Letters in applied microbiology 2003, 37(6):438-42.
21. Pinheiro R, Belo II, Mota M. Air pressure effects on biomass yield of two different Kluyveromyces strains. Enzyme and microbial technology 2000, 26(9-10):756-62.
22. Castillo H, Li X, Schilkey F, Smith GB. Transcriptome analysis reveals a stress response of Shewanella oneidensis deprived of background levels of ionizing radiation. PloS one 2018, 13(5):e0196472.
23. Zhou X, Liao W-J, Liao J-M, Liao P, Lu H. Ribosomal proteins: functions beyond the ribosome. Journal of Molecular Cell Biology, 7(2):92-104.
24. Sonenberg N, Hinnebusch AG. Regulation of Translation Initiation in Eukaryotes: Mechanisms and Biological Targets. 136(4):0-745.
25. Choi WG, Han J, Kim J-H, Kim M-J, Park J-W, Song B, Cha H-J, Choi H-S, Chung H-T, Lee I-K. eIF2α phosphorylation is required to prevent hepatocyte death and liver fibrosis in mice challenged with a high fructose diet. Nutrition & Metabolism, 14(1):48.
26. Merchante C, Stepanova AN, Alonso JM. Translation regulation in plants: an interesting past, an exciting present and a promising future. The Plant journal : for cell and molecular biology 2017, 90(4):628-53.
27. Wellmann S, Truss M, Bruder E, Tornillo L, Zelmer A, Seeger K, Bührer C. The RNA-Binding Protein RBM3 Is Required for Cell Proliferation and Protects Against Serum Deprivation-Induced Cell Death. 2010, 67(1):35.
28. Liao Y, Tong L, Tang L, Wu S. The Role of Cold-inducible RNA binding protein (CIRP) in Cell Stress Response. International Journal of Cancer.
29. Fan NJ, Gao JL, Liu Y, Song W, Zhang ZY, Gao CF. Label-free quantitative mass spectrometry reveals a panel of differentially expressed proteins in colorectal cancer. BioMed research international 2015, 2015:365068.
30. Bennett GR, Ryan P, Xiao-hong W, Jeungphill H, W. SR, Ralf B, Richard F, E. YK, Maria S. Repair of Oxidative DNA Base Damage in the Host Genome Influences the HIV Integration Site Sequence Preference. PloS one, 9(7):e103164-.
31. Bjelland S, Seeberg E. Mutagenicity, toxicity and repair of DNA base damage induced by oxidation. 531(1-2):37-80.
32. Chatterjee N, Walker GC. Mechanisms of DNA damage, repair, and mutagenesis. Environmental and molecular mutagenesis 2017, 58(5):235-63.
33. Chien CY, Hung YJ, Shieh YS, Hsieh CH, Lee CH. A novel potential biomarker for metabolic syndrome in Chinese adults: Circulating protein disulfide isomerase family A, member 4. PloS one 2017, 12(6):e0179963.
34. Qi L, Wu P, Zhang X, Qiu Y, Jiang W, Huang D, Liu Y, Tan P, Tian Y. Inhibiting ERp29 expression enhances radiosensitivity in human nasopharyngeal carcinoma cell lines. Medical oncology (Northwood, London, England) 2012, 29(2):721-8.
35. Winship AL, Sorby K, Correia J, Rainczuk A, Yap J, Dimitriadis E. Interleukin-11 up-regulates endoplasmic reticulum stress induced target, PDIA4 in human first trimester placenta and in?vivo in mice. Placenta, 53:92-100.
36. Vig S, Buitinga M, Rondas D, Crevecoeur I, van Zandvoort M, Waelkens E, Eizirik DL, Gysemans C, Baatsen P, Mathieu C et al. Cytokine-induced translocation of GRP78 to the plasma membrane triggers a pro-apoptotic feedback loop in pancreatic beta cells. Cell Death Dis 2019, 10(4):309.
37. Kaur G, Singh S, Dutta T, Kaur H, Singh B, Pareek A, Singh P. The peptidyl-prolyl cis-trans isomerase activity of the wheat cyclophilin, TaCypA-1, is essential for inducing thermotolerance in Escherichia coli. 2016, 2(C):9-15.
38. Tork Ladani S, Souffrant MG, Barman A, Hamelberg D. Computational perspective and evaluation of plausible catalytic mechanisms of peptidyl-prolyl cis–trans isomerases. Biochimica Et Biophysica Acta, :S0304416515000185.
39. Youle RJ, van der Bliek AM. Mitochondrial fission, fusion, and stress. Science 2012, 337(6098):1062-5.
40. Lu Z, Wang S, Ji C, Li F, Cong M, Shan X, Wu H. iTRAQ-based proteomic analysis on the mitochondrial responses in gill tissues of juvenile olive flounder Paralichthys olivaceus exposed to cadmium. Environmental pollution (Barking, Essex : 1987) 2019, 10.1016/j.envpol.2019.113591:113591.
41. Hsu FS, Spannl S, Ferguson C, Hyman A, Parton RG, Zerial M. Rab5 and Alsin regulate stress-activated cytoprotective signaling on mitochondria. 2018, 7.
42. Huang L, Huang L, Zhao L, Qin Y, Su Y, Yan Q. The regulation of oxidative phosphorylation pathway on Vibrio alginolyticus adhesion under adversities. MicrobiologyOpen 2019, 8(8):e00805.

Supplementary Files Legend

Additional files

Additional file 1: S Table1. The total differentially abundant proteins. (XLSX 61 kb)

Additional file 2: S Table2. GO analyses result of differentially abundant proteins.(XLSX 11 kb)

Additional file 3: Stable 3.Differentially abundant proteins verificated by Parallel Reaction Monitoring.(XLSX 12 kb)

Additional file 4: Stable 4. PPI network.(XLSX 53 kb)

Figures

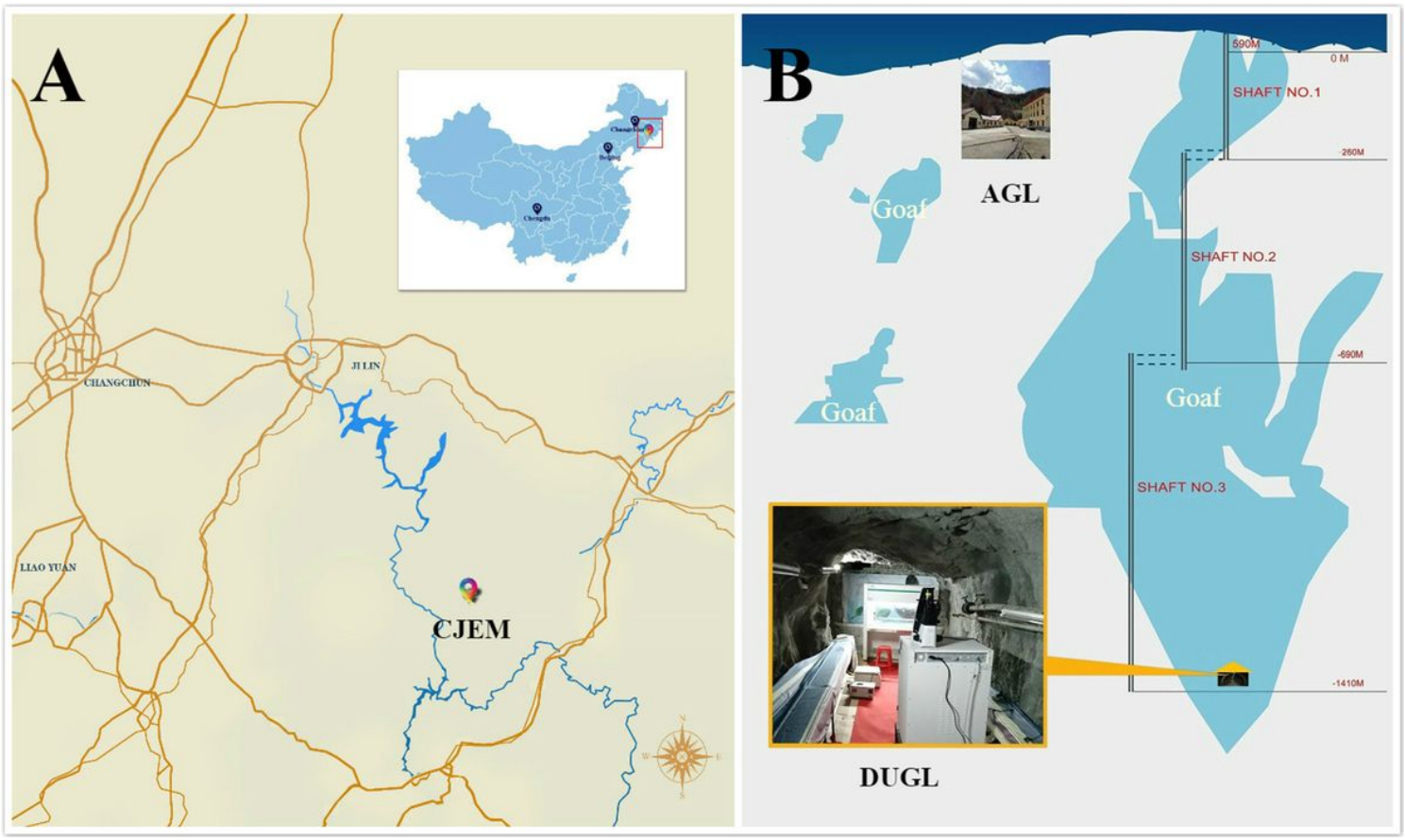

Figure 1

The location of the DUGL and the AGL at the CJEM. The location of the CJEM in China (A), and the location of the DUGL and the AGL in the CJEM (B). AGL, above-ground laboratory; CJEM, Erdaogou Mine, Jiapigou Minerals Limited Corporation of China National Gold Group Corporation; DUGL, deep-underground laboratory. Note: The designations employed and the presentation of the material on this map do not imply the expression of any opinion whatsoever on the part of Research Square concerning the legal status of any country, territory, city or area or of its authorities, or concerning the delimitation of its frontiers or boundaries. This map has been provided by the authors.

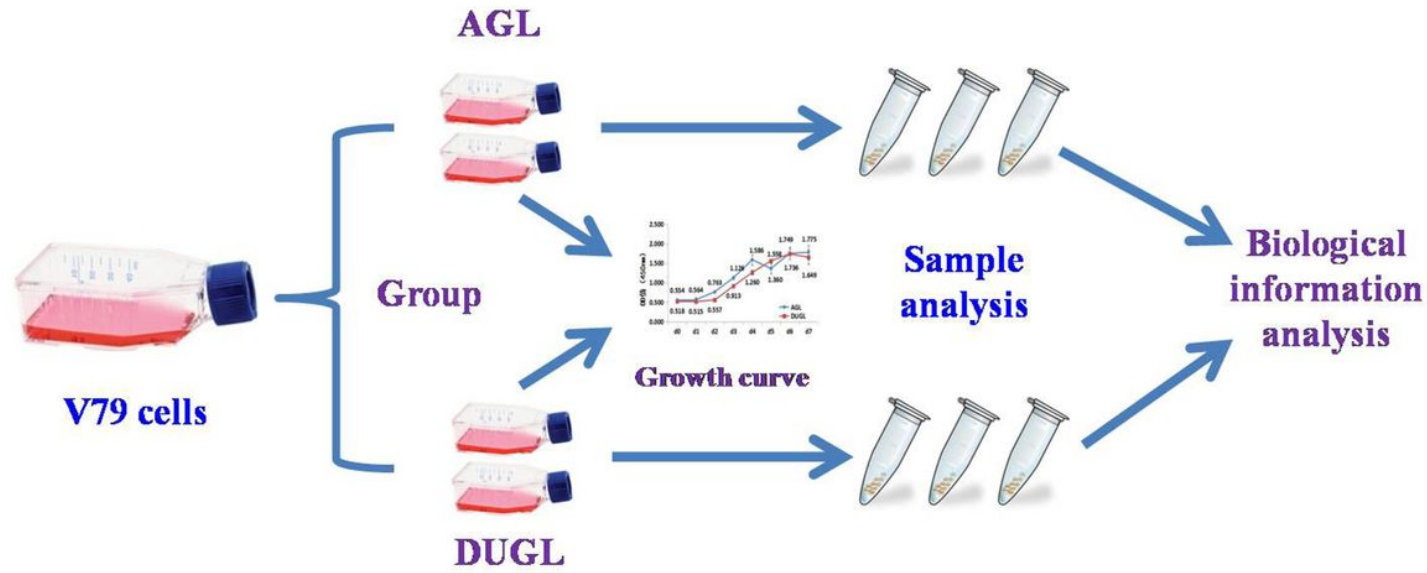

Figure 2

Flow chart showing the study design

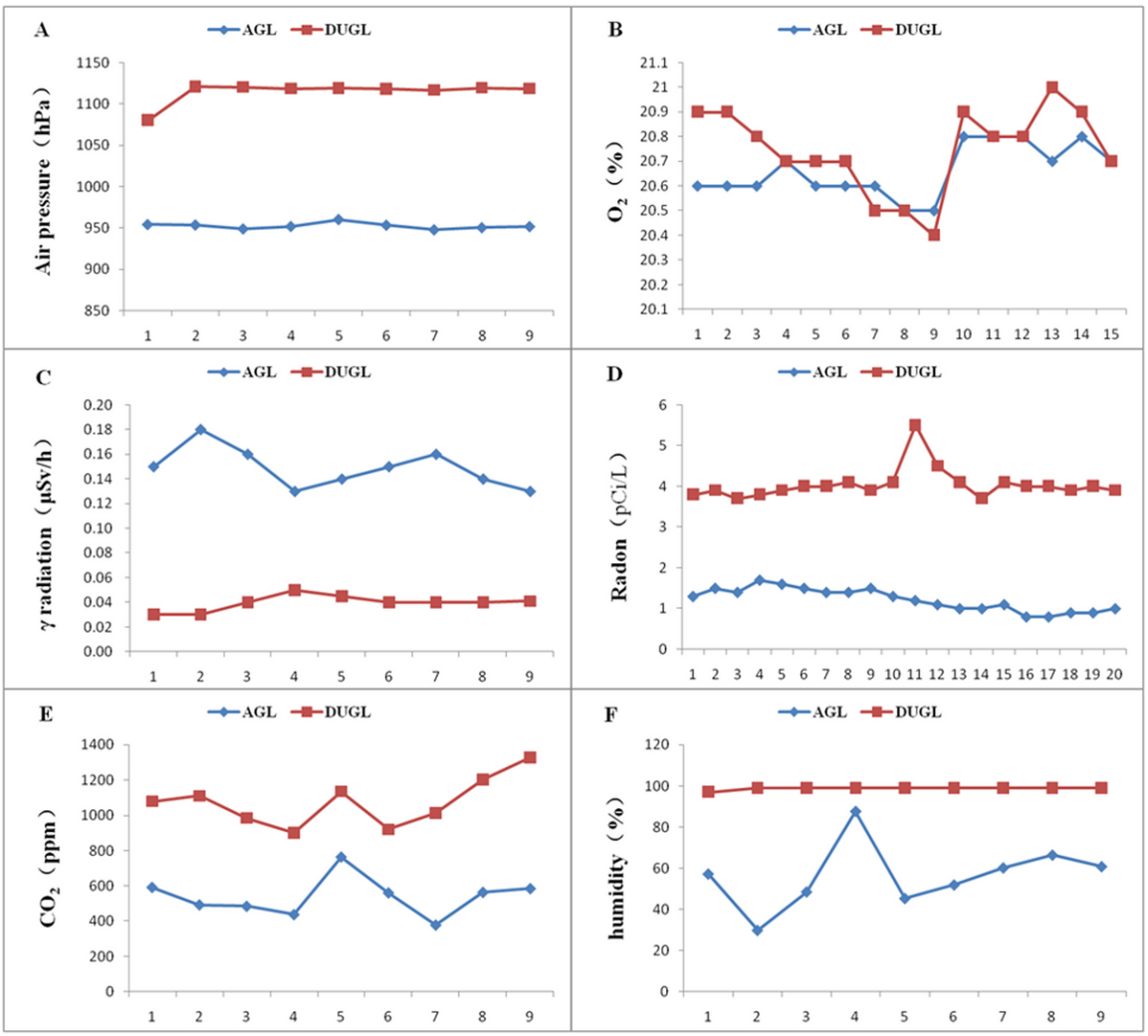

Figure 3

Variations in the environmental characteristics in the DUGL and AGL. AGL, above-ground laboratory; DUGL, deep underground laboratory

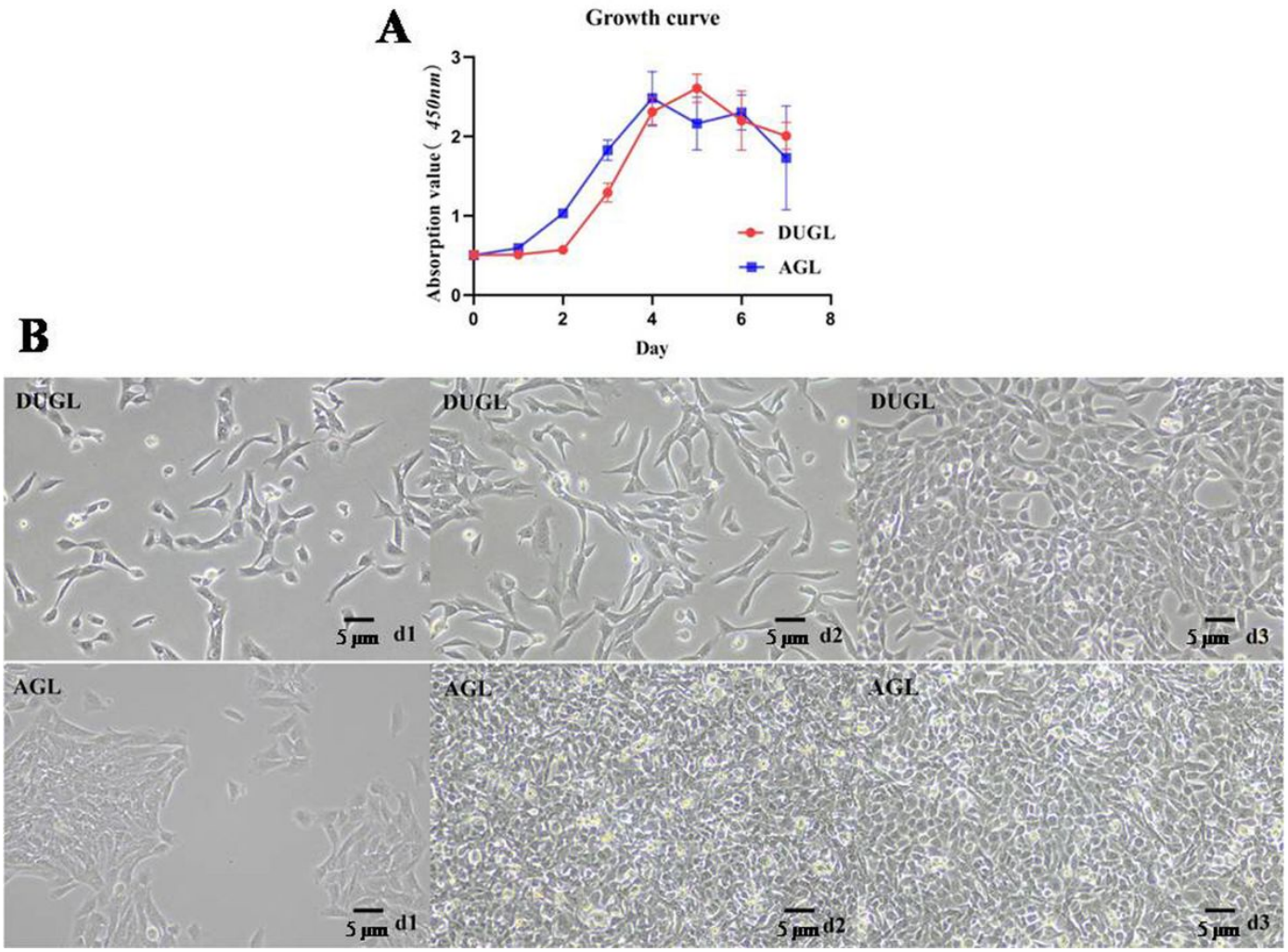

Figure 4

Growth curves of V79 cells cultured in the DUGL or AGL (A). V79 cells cultured for 3 days in the DUGL or AGL observed by light microscopy 10× (B). AGL, above-ground laboratory; DUGL, deep underground laboratory

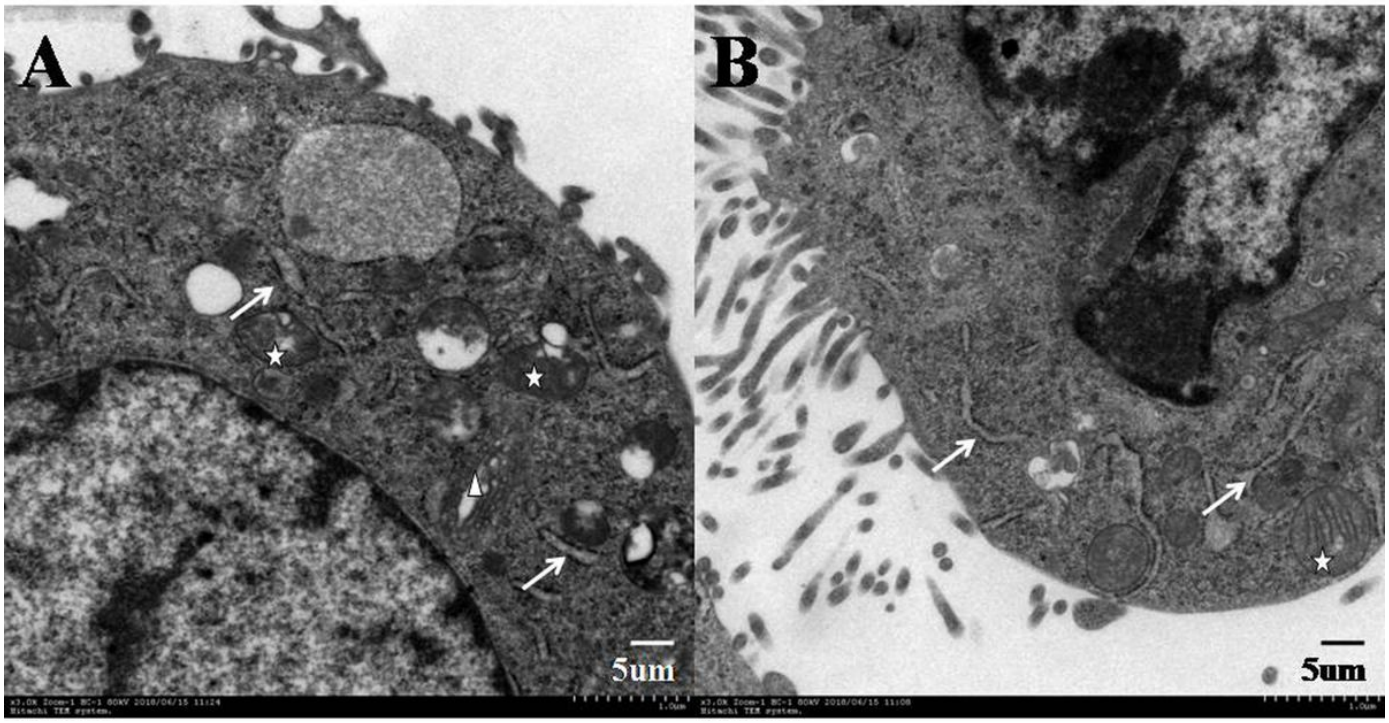

Figure 5

Transmission electron microscopy of V79 cells cultured in the AGL (B) or DUGL (A) 3000× White arrows: endoplasmic reticulum;▯: mitochondria;△: Golgi body. AGL, above-ground laboratory; DUGL, deep underground laboratory

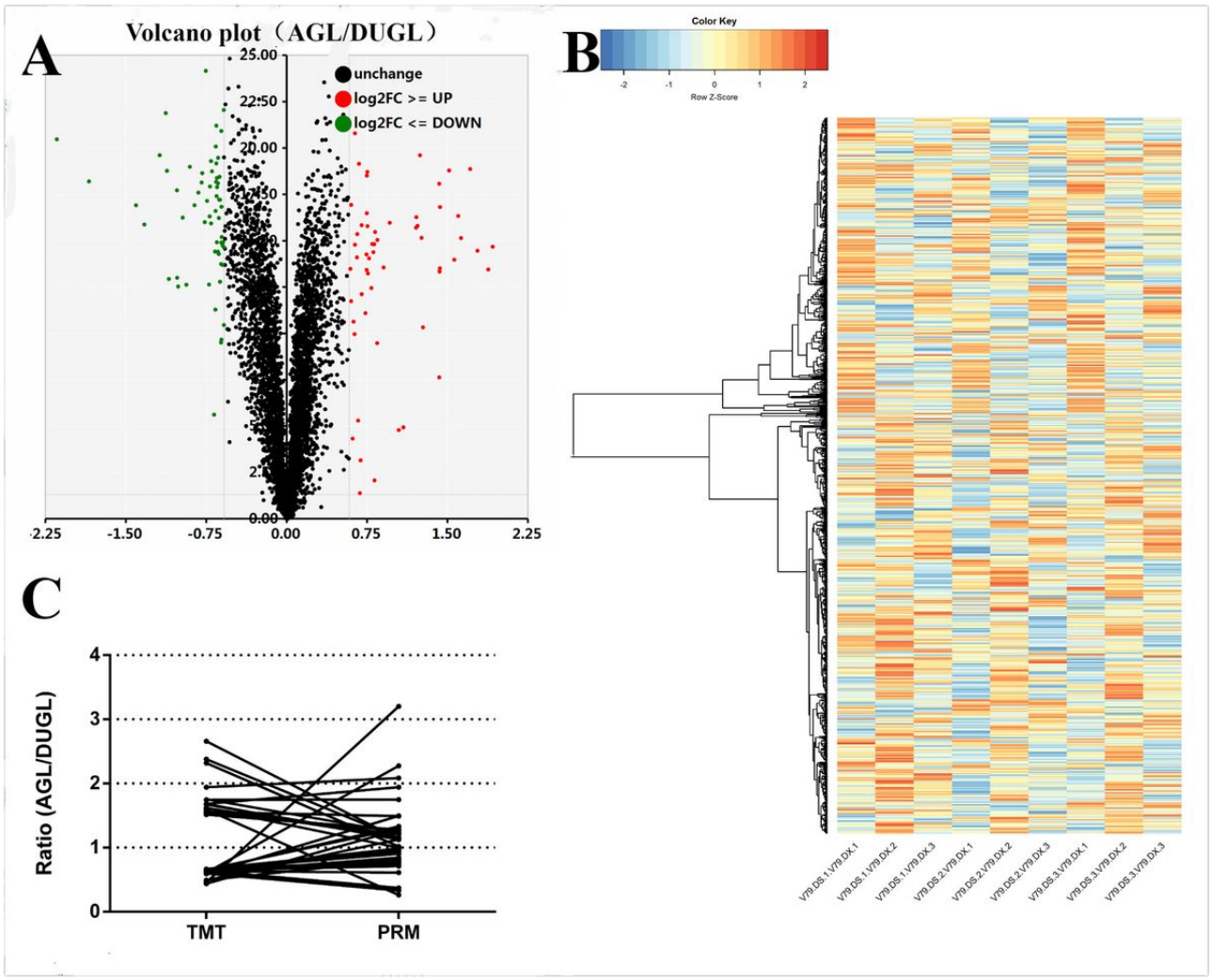

Figure 6

Volcano plot (red, up-regulated DAPs; black, unchanged DAPs; green, down-regulated DAPs [AGL/DUGL]) (A) and hierarchical cluster (white, unchanged DAPs; bright red, over-expression of DAPs [AGL/DUGL]) (B) of DAPs in V79 cells cultured in the DUGL. Verification analysis shows selected DAPs verified by PRM (AGL/DUGL) (C). DAP, differentially abundant proteins; DUGL, deep underground laboratory; AGL, above ground laboratory; PRM, parallel reaction monitoring

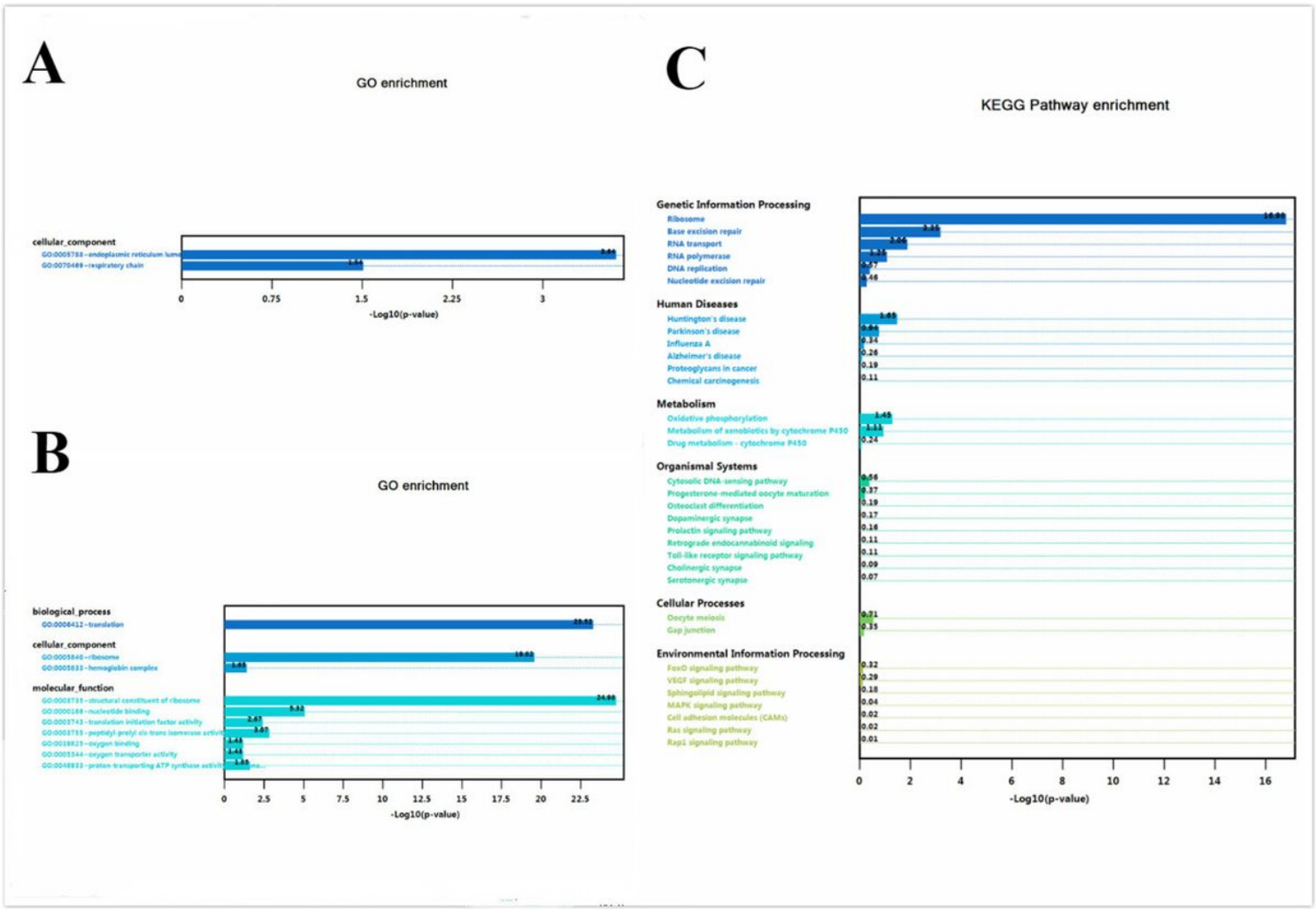

Figure 7

GO enrichment analysis of down-regulated proteins (A) and up-regulated proteins (B) inV79 cells cultured in the DUGL. (C) KEGG pathway analysis. DUGL, deep underground laboratory; GO, gene ontology; KEGG, Kyoto Encyclopedia of Genes and Genomes

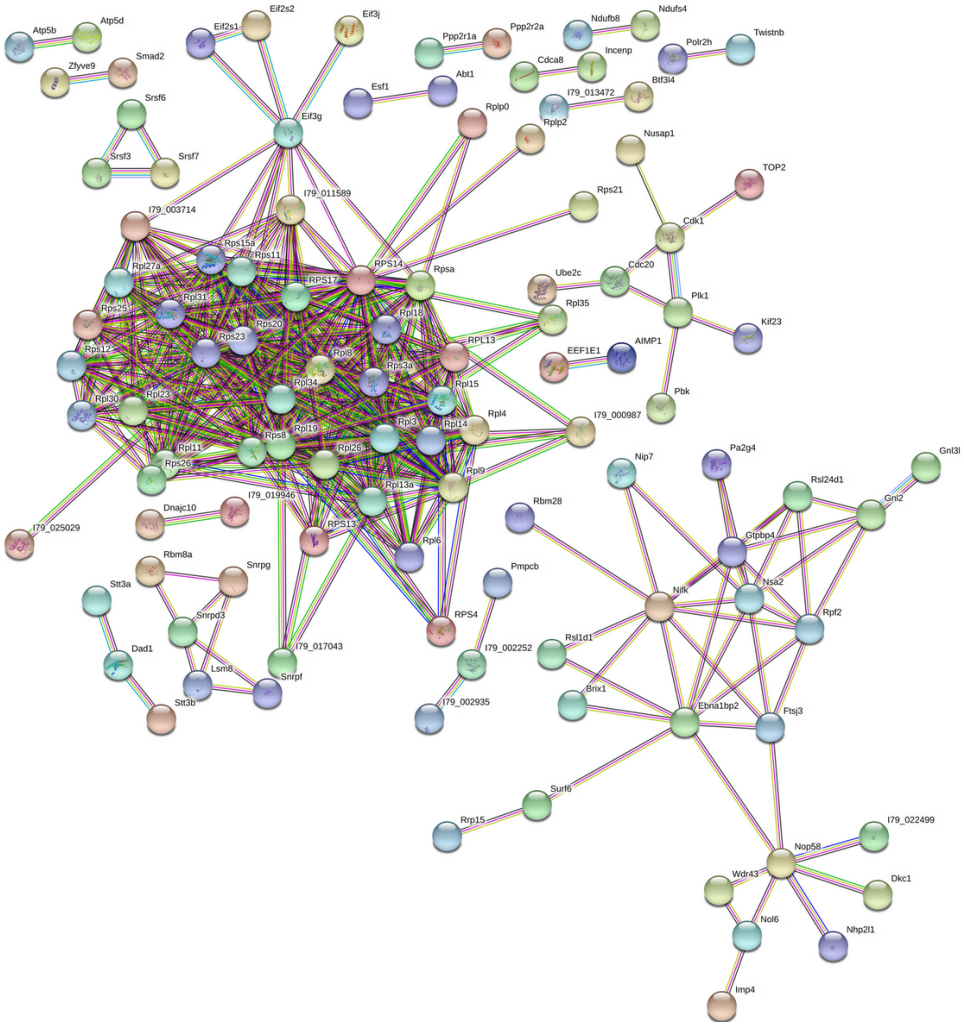

Figure 8

Protein-protein interaction network of DAPs in V79 cells. DAP, differentially abundant proteins

Supplementary Files

This is a list of supplementary files associated with this preprint. Click to download.

- Stable2.GOanalysesresultofDAPs.xlsx
- Stable1.Thetotaldifferentiallyabundantproteins.xlsx
- Stable4PPInetwork.xlsx
- Stable3.DAPsverificatedbyParallelReactionMonitoring.xlsx